Algal Research 31 (2018) 47–59

Contents lists available at ScienceDirect

Algal Research

journal homepage: www.elsevier.com/locate/algal

Cultivation of *Emiliania huxleyi* for coccolith production

I. Jakob*, F. Weggenmann, C. Posten

Karlsruher Institut für Technologie (KIT), Institut für Bio-und Lebensmitteltechnik III: Bioverfahrenstechnik, Germany

1. Introduction

Coccoliths from coccolithophorid microalgae possess a sophisticated three-dimensional architecture while being monodisperse at the same time [1–4]. This quality is derived from strictly controlled intracellular biomineralization, which cannot be reproduced synthetically [5,6]. The coccolithophorid species *Emiliania huxleyi* (Lohm.) Hay and Mohler (Prymnesiophyceae) has been intensively studied for being the most abundant calcite producing microorganism in the ocean [7,8]. Fixing inorganic CO_2 by photosynthesis and biomineralization contributes significantly to global carbon cycling with 1–10% [9]. In nature, an *Emiliania huxleyi* (*E. huxleyi*) cell is usually covered with a coccosphere consisting of 10–15 coccoliths. Coccoliths are produced even when the cells are not actively growing [10], with an approximate rate of 1–2 h^{-1} under optimum conditions [11]. Surprisingly, the biological functions of coccoliths are still being debated [12,13].

Coccoliths exhibit various interesting characteristics. They are not purely inorganic but possess organic molecules on the surface and embedded in the coccolith material. These are the remains of the organic matrix involved in biomineralization control [14–16]. Because of its organic skeleton, coccoliths are more robust in calcium-free solution and pure water compared to synthetic calcite particles [17]. Structural micropores and nanopores facilitate a large specific surface area of roughly 20 $m^2 g^{-1}$ [4]. Coccoliths also exhibit exceptional optical features. Coccosphere-covered cells show a transition of structural color under the influence of a strong magnetic field [18]. The intensity of light scattering from a coccolith suspension is also magnetically alterable [19].

These unique properties could be exploited for multiple applications. Coccoliths have found potential applications in paper manufacturing, colors and lacquers, heterogeneous catalysis, drug delivery, composite materials, heavy metal binding, optical applications and transplant materials [4,20,21]. Furthermore, it was already demonstrated that coccoliths are feasible enzyme carriers [22].

Despite its robust potentials, coccoliths have surprisingly received little attention and no ideas regarding their application have been further pursued. One easy explanation is the lack of adequate material quantities. While tons of calcite particles are easily produced from grinding limestone or precipitation every day, non-fossil coccoliths are hard to harvest from the ocean in sufficient amounts. This might not seem obvious since *E. huxleyi* can cover large areas during blooms. The actual cell concentrations are, however, rather low with approximately 10^3 cells mL^{-1} [7]. Thus, ocean water contains coccoliths in the milligrams per liter scale mixed with other unwanted phytoplankton.

Coccolithophorid mass cultivation, on the other hand, can potentially provide large amounts of intact, single-variety coccoliths. A desirable process should yield several g L^{-1} of coccoliths. This demands cell concentrations that are roughly 10.000–100.000 times higher than those present in the ocean. Unfortunately, there has been modest interest in coccolithophorid mass cultivation and therefore limited documented experience. Moheimani et al. cultivated several coccolithophorid species in different closed photobioreactors (PBRs) in repeated batch-mode [23]. Although satisfactory growth rates of about 1.0 d^{-1} were achieved in some systems, $r_{P,V}$ was roughly 0.06 g L^{-1} d^{-1} [23]. Takano et al. investigated the cultivation of *Emiliania huxleyi* and *Pleurochrysis carterae* [24–27]. They were able to harvest approximately 0.7 g L^{-1} of coccoliths from DIC- enriched batch-cultures [26]. This is the highest coccolith concentration reported in literature so far. Promising coccolith productivities of 0.27 g L^{-1} d^{-1} were achieved in nutrient enriched repeated-batch cultures [26]. In the long term, it is no practical option to produce coccoliths in repeated-batch mode and to concurrently replenish four substrates.

In this study, we developed a comprehensive cultivation strategy for coccolith production in a batch-mode system. Strains of *E. huxleyi* can express extensive genetic variations [28]. Process development must therefore be approached from various angles and optimized for a specific strain.

1.1. Nutrient availability

E. huxleyi is commonly cultured in enriched natural seawaters or artificial seawaters like ESAW (Enriched Seawater, Artificial Water) [29]. Although it can be easily cultivated in the lab, it does not usually grow beyond 1–5 10^6 cells mL^{-1} [30,31]. One obvious explanation is the depletion of major substrates like phosphorous. Previous studies involving *E. huxleyi* cultivation were carried out at cell concentrations

Abbreviations: $CaCO_3$, calcium carbonate mineral; CO_2, carbon dioxide; cBPB, costum-built pilot bag photobioreactor; DIC, dissolved inorganic carbon; HCO_3^-, bicarbonate; NO_3^-, nitrate; Ω, saturation state of a mineral; PBR, photobioreactor; PFD, photon flux density; PO_4^{3-}, phosphate; pCO_2, carbon dioxide partial pressure; $\mathbf{pCO_{2,\,const}}$, controlled carbon dioxide partial pressure; $\mathbf{pCO_{2,inital}}$, initial carbon dioxide partial pressure; $\mathbf{r_{P,C}}$, average cellular productivity; $\mathbf{r_{P,V}}$, volumetric productivity; $\mathbf{r_X}$, uptake rate of substrate X; **TA**, total alkalinity

* Corresponding author.
E-mail addresses: ioanna.jakob@kit.edu (I. Jakob), clemens.posten@kit.edu (C. Posten).

https://doi.org/10.1016/j.algal.2018.01.013
Received 5 October 2017; Received in revised form 13 December 2017; Accepted 25 January 2018
Available online 03 February 2018

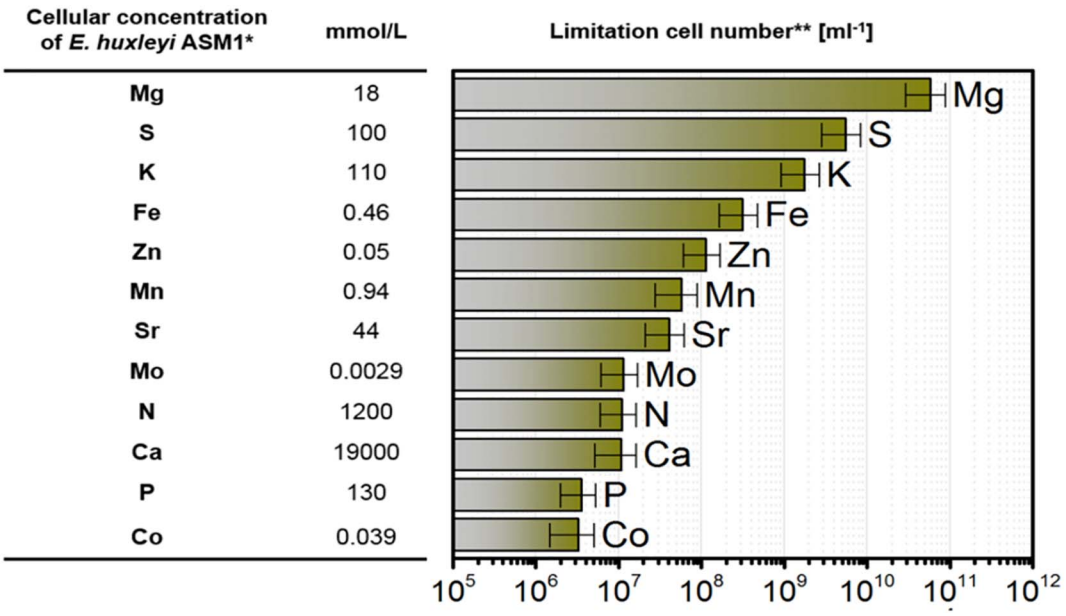

Fig. 1. Limitation model of *Emiliania huxleyi* maximum cell concentration in ESAW based on data from Ho et al. [80]. *Cellular element concentration, normalized to cellular volume. **Limitation cell number for cultivation in ESAW medium based on the cellular concentration. Values derive from calculation with an average symplast radius of 2.25 ± 0.25 µm (n = 200) (see Supplement A).

well below 1 10^6 cells mL^{-1} in order to avoid mutual shading or by-product formation. Since improving final cell concentration was not the primary objective of most of the studies, alternative media with enhanced nutrient composition have yet to be developed.

In order to increase cell concentration by medium optimization, a close look must be taken at all essential medium components, their stoichiometric presence in the organism and their consumption over time. Fig. 1 shows the theoretically possible concentration of *E. huxleyi* cells in ESAW medium, as calculated from the elemental cell composition of the strain ASM1. Without any recipe alteration, the culture is subject to phosphorous limitation at 1–5 10^6 cells mL^{-1}. Phosphorous and nitrogen are crucial not only for growth but also for calcification [30–33]. ESAW already contains much more nitrogen and phosphorous (550 µmol L^{-1} N and 21 µmol L^{-1} P) than natural seawater (0–25 µmol L^{-1} N and 0–2 µmol L^{-1} P [34]). Adding further N- and P sources seems like a suitable starting point. Takano et al. was able to achieve an increase in cell concentration of *E. huxleyi* 92D to $2{\cdot}10^7$ cells mL^{-1} by N- and P enrichment and addition of $NaHCO_3$ as C-source [26]. Unfortunately, there is still incomplete knowledge about N- and P inhibition in *E. huxleyi*. It is therefore difficult to estimate to what extent the initial substrate concentrations in the medium may be raised. Another nutrient present in the cell in comparably large amounts is Strontium (Sr). Taking cell stoichiometry into account, Sr may be depleted, even if N- and P sources are still sufficiently present. The role of Sr in *E. huxleyi* is poorly understood. It supports biomineralization [35] and is present in the coccolith material in different amounts [4,36]. *E. huxleyi* only requires low concentrations of several metals [37], such as Co and Mo, to grow beyond 10^8 cells mL^{-1}. This effect could be partly explained by the ability of the cells to replace trace metals through certain metabolic functions [38]. To avoid growth limitation due to substrate depletion, it is a logical step to adapt the recipe of the culture medium. Limitation as well as substrate inhibition and precipitation must be avoided at the same time. Substrates which cannot be increased in the initial concentration must be replenished before they are depleted, or better, supplied continuously by automated feeding. This probably applies to calcium. Calcium is a potent intracellular messenger and is known to inhibit growth and calcification above 20 mM [39]. For batch-processes, it is worth investigating novel strategies for increased calcium supply without inhibition. Slow-release substrates have already been tested in other fields of biotechnology [40] and could also be established in coccolithophorid cultivation.

1.2. Carbon availability and carbonate chemistry

The uptake and utilization of carbon is probably the most intensively studied topic within *E. huxleyi* research and has been summarized in several comprehensive reviews [16,41–43]. For process development, it is important to understand the requirements for calcification and the feedback effects on the medium. *E. huxleyi* uses solely HCO_3^- as DIC source for calcification and mainly CO_2 for growth. HCO_3^- is used under CO_2 deplete conditions, although less efficiently [44–47]. Therefore, cells constantly take up dissolved inorganic carbon from the medium. The consumed carbon must be replaced or growth and calcification come to a halt. One option for carbon replenishment is to supply inorganic carbon directly by adding $NaHCO_3$ [26]. Another option is to bubble the culture with CO_2. This method is easier to set up and much more commonly used in lab cultivations. Bubbling with CO_2 is especially elegant as it can be used to control pH in cultivations where pH otherwise tends to rise. However, the situation is more difficult with coccolithophorid cultivation. Coccolith formation causes the release of protons [48] resulting in pH drop during cultivation. Consequently, less inorganic carbon remains in solution and $\Omega CaCO_3$ decreases to < 1 at a certain point [49]. Under this condition, the medium is undersaturated and the equilibrium favors the dissolution of coccoliths instead of their formation [49–51]. This may lead to a different quality of coccoliths within one batch or even malformations, especially in the later stages of cultivation [52]. Instead, a carbonate system able to maintain a constant carbon concentration even at high cell densities and coccolith production rates is desirable. In a PBR, this can be technically implemented by the simultaneous control of dissolved pCO_2 and pH. While pH is maintained mainly by titration with NaOH, dissolved pCO_2 is controlled by adjusting the concentration of CO_2 in the influent gas.

1.3. Light supply

Growth and calcification are both light-dependent processes [53–55]. Studies performed over the last decades have investigated the

impact of light, irradiance and wavelength on *E. huxleyi* cultures [54,56–58]. The individual reports, however, delivered divergent results. This may be due to differences in the pigment composition of the investigated strains [59]. In addition, the different methods used to measure and adjusting irradiance complicate any comparison. *E. huxleyi* has previously been reported to display no signs of light inhibition at full daylight [60]. For this reason, this alga has often been considered to be extremely light-tolerant. We have, however, recently demonstrated that *E. huxleyi* RCC1216 has a much narrower range of optimum photon flux density between 100 and 500 µmol $m^{-2} s^{-1}$ [61]. Growth was inhibited at higher irradiances, even after months of adaptation time. These results underscore the species-specific nature of light dependency. Optimal light conditions therefore have to be determined individually for every strain.

1.4. Low-shear mixing and aeration

The mixing regime of a bioreactor is an important cultivation parameter [62]. It is responsible for the homogeneous distribution of nutrients, carbon, suspended cells and gas exchange. Langer et al. proposed the correlation between unequal distribution of nutrients due to inadequate mixing with the malformation of coccoliths [63]. At the same time, there is a limit to the level of mixing that can be applied to the microalgal culture. Stronger mixing increases hydrodynamic forces and leads to shear stress. Aeration can also cause shear stress. Cell damage during sparging is commonly associated with the break-up of bubbles at the surface [64] and with the formation of bubbles at the sparger [65]. *E. huxleyi* was indeed reported to be sensitive to bubble aeration [23].

A successful strategy to produce significant amounts of coccoliths must take into account all of the listed challenges associated with *E. huxleyi* cultivation and address them within a single process. In this study, we developed a lab-scale cultivation system capable of producing several g L^{-1} of high-quality intact coccoliths. To achieve this primary objective, we tailored the composition of the common cultivation medium ESAW to support *E. huxleyi* specific growth requirements, tested an alternative slow-release substrate for $CaCl_2$ replenishment and evaluated two different carbonate system working points. Finally we transferred our lab-scale approach to a costum-built pilot bag photobioreactor (cBPB), to lay the foundation for future large-scale production of coccoliths.

2. Material and methods

2.1. Shake flask cultivations

Axenic cultures of *Emiliania huxleyi* RCC1216 (Roscoff Culture Collection, France) were grown in 500 mL conical flasks containing 200 mL medium and incubated at 21 °C in a climate chamber. Light was provided from the flask bottom by a panel containing warm-white LEDs (Nichia NS67L183BT). Irradiance was adjusted by measurement of the photon flux density on the shake flask bottom with a planar light Sensor (Li-250, Li-Cor). Irradiance was set at 350 µmol $m^{-2} s^{-1}$ in all experiments. The panel with the culture flasks was agitated by an orbital shaker (IKA KS501) at 100 rpm and a shaking diameter of 30 mm. Precultures were cultivated under the same conditions as the main experiments for at least seven days. Prior to inoculation of main cultures, axenicity was checked by light microscopy and by sub-cultivation onto agar plates, which supported the growth of both bacteria and fungi. All media were sterilized for 21 min at 2 bar and 121 °C in pressure-tight laboratory bottles, to prevent outgassing of dissolved CO_2. NaH_2PO_4, $NaNO_3$ and $CaCl_2$ were added from sterile stock solutions after autoclaving. Main cultures were inoculated with an initial cell concentration of 10^4 mL L^{-1}. All shake flask experiments were performed in biological triplicates.

2.1.1. Replenishment of dissolved inorganic carbon and nutrients

Batch cultures were grown in enriched seawater, artificial water (ESAW) medium [29], containing 1.34 g L^{-1} $CaCl_2{\cdot}2H_2O$ (366 mg L^{-1} Ca^{2+}), 46.7 mg L^{-1} $NaNO_3$ (34 mg L^{-1} NO_3^-), 3.09 mg L^{-1} $NaH_2PO_4{\cdot}H_2O$ (2.0 mg L^{-1} PO_4^{3-}), 21.8 mg L^{-1} $SrCl_2{\cdot}6H_2O$ (7.0 mg L^{-1} Sr^{2+}) and 0.174 g L^{-1} $NaHCO_3$. The medium composition provided an initial total alkalinity (TA) of 2300 µmol kg^{-1}. In DIC replenished cultures, TA was used as a reference and was daily refilled to a target value of 2000 µmol kg^{-1} by adding $NaHCO_3$ stock solution (4.2 g L^{-1}/42 g L^{-1}; 1 mol HCO_3 equals 1 mol TA [66]). In order to prevent limitation, target values were raised to 4600 µmol kg^{-1} when consumption rates exceeded 2000 µmol kg^{-1} d^{-1}. The daily concentration of NO_3^-, PO_4^{3-} and Ca^{2+} was determined photometrically. In substrate replenished cultures, sterile stock solutions of $NaH_2PO_4{\cdot}H_2O$ (0.63 g L^{-1}/6.3 g L^{-1}), $NaNO_3$ (9.88 g L^{-1}/42.734 g L^{-1}/362.65 g L^1) and $CaCl_2{\cdot}2H_2O$ (500 g L^{-1}) were used to refill the single substrates according to Table 1.

2.1.2. Variation of initial substrate concentrations

Batch cultures were grown in ESAW medium with different initial concentrations of $NaH_2PO_4{\cdot}H_2O$ (2.0, 10.0, 20.0, 100.0 and 200.0 mg L^{-1} PO_4^{3-}), $NaNO_3$ (34.0, 170.0, 340.0, 1700.0 and 3400.0 mg L^{-1} NO_3^-), $SrCl_2{\cdot}6H_2O$ (7.0, 14.0, 35.0 and 70.0 mg L^{-1} Sr^{2+}), and $CaCl_2{\cdot}2H_2O$ (66.0, 132.0, 330.0 and 660 mg L^{-1} Ca^{2+}).

2.1.3. $CaCO_3$ as an alternative substrate to deliver carbon and Ca^{2+}

Cultures were grown in ESAW medium containing 77.3 mg L^{-1} $NaH_2PO_4{\cdot}H_2O$ (25-fold) and 545 mg L^{-1} $NaNO_3$ (25-fold). 1 g L^{-1} $CaCO_3$ was added to the medium recipe replacing $CaCl_2$.

2.2. Photobioreactor setup and experimental conditions

Cultivations were carried out in a 2-L stirred photobioreactor (Bioengineering KLF 2000), operated with the software BioProCon (in-house development). The reactor had a working volume of 1.6 L and was equipped with two rushton turbines for culture homogenization.

Table 1
Scheme for substrate replenishment in parallel shake flask cultures. Cultivations were conducted in triplicates.

Culture (n = 3)	Daily refill	Target concentration (ESAW)			
		Total alkalinity	NO_3^-	PO_4^{3-}	Ca^{2+}
		µmol kg^{-1}	mg L^{-1}	mg L^{-1}	mg L^{-1}
Control	–	–	–	–	–
+ HCO_3^-	$NaHCO_3$	2300/4600	–	–	–
+ HCO_3^-, NO_3^- PO_4^{3-}	$NaHCO_3$, $NaNO_3$, $NaH_2PO_4{\cdot}H_2O$	2300/4600	34.0	2.0	–
+ HCO_3^-, NO_3^- PO_4^{3-}, Ca^{2+}	$NaHCO_3$, $NaNO_3$, NaH_2PO_4 $NaH_2PO_4{\cdot}H_2O$, $CaCl_2{\cdot}2H_2O$	2300/4600	34.0	2.0	366
+ HCO_3^-, NO_3^-, PO_4^{3-},Ca^{2+}	$NaHCO_3$, $NaNO_3$, NaH_2PO_4 $NaH_2PO_4{\cdot}H_2O$, $CaCl_2{\cdot}2H_2O$	2300/4600	34.0	2.0	36.6
+ HCO_3^-, NO_3^- PO_4^{0033-},Ca^{2+}	$NaHCO_3$, $NaNO_3$, NaH_2PO_4 $NaH_2PO_4{\cdot}H_2O$, $CaCl_2{\cdot}2H_2O$	2300/4600	34.0	2.0	732

The cultures were stirred with 150 rpm at 21 °C. A customized cylindrical LED-cover with warm white LEDs (Nichia NS6L083AT, surface-mounted) was used for illumination. In all cultivations, irradiance level inside the culture vessel was set at 350 µmol $m^{-2} s^{-1}$. Medium pH and dissolved pCO_2 were controlled by two separate systems. pH was measured with an online probe (Hamilton, Polylite plus) and adjusted by titration with 2 M NaOH and 2 M HCl. A pI-controller was used for $pCO_{2,const}$ regulation. This included a pCO_2 probe (Mettler Toledo InPro5000i) for continuous online measurement of dissolved pCO_2 and mass flow controllers for defined air (MKS Instruments, 1179B) and CO_2 (MKS Instruments, M330) supply. Aeration was performed by headspace gas flushing of air/CO_2 mixtures with 0.05 vvm. Prior to all experiments medium without NaH_2PO_4, $NaNO_3$ and $CaCl_2$ was sterilized in-situ for 21 min at 121 °C. These substrates were later added after sterilization from sterile stock solutions. The medium was saturated to target $pCO_{2,const}$-setpoints before inoculation. Samples were taken daily through a sampling port at the bottom of the reactor.

2.2.1. Low carbon scenario cultivations

Cells were grown at $pCO_{2,const}$ of 0.04–0.06% and pH 8.2 in ESAW medium without alterations to its original recipe, resembling the approximate carbonate distribution in the ocean. A second cultivation was conducted under identical conditions but with daily replenishment of NO_3^-, PO_4^{3-} and Ca^{2+} (34 mg L^{-1} NO_3^-, 2.0 mg L^{-1} PO_4^{3-} and 66 mg L^{-1} Ca^{2+}).

2.2.2. High carbon scenario cultivation

Cells were grown at a pH 8.0 and $pCO_{2,initial}$ of 1%. In this case, the dissolved pCO_2 was not controlled. Instead, the culture medium was continuously aerated with air containing 1% CO_2. This should allow the carbonate system to drift during the cultivation. NO_3^-, PO_4^{3-} and Ca^{2+} concentrations were measured and replenished to their initial values on a daily basis (34 mg L^{-1} NO_3^-, 2.0 mg L^{-1} PO_4^{3-} and 36.6 mg L^{-1} Ca^{2+}).

2.2.3. Cultivation in a controlled high-carbon environment and use of a modified medium

Cells were grown in modified ESAW medium (ESAW*, see Supplement B), which contained a 25-fold initial $NaNO_3$ (850 mg L^{-1} NO_3^-) a 25-fold initial NaH_2PO_4 (50 mg L^{-1} PO_4^{3-}), a 5-fold SrCl (35 mg L^{-1} Sr^{2+}) and a 5-fold initial trace elements concentration. NO_3^-, PO_4^{3-} and Ca^{2+} were daily measured and refilled before depletion. As soon as the culture showed a reduction of cell concentration at the end of the stationary phase, PFD was adjusted to 2000 µmol $m^{-2} s^{-1}$ in order to terminate the cultivation.

A second cultivation was performed under the same conditions but with 10-fold reduced $Na_2SiO_3 * 5H_2O$ (0.97 mg L^{-1} SiO_4^{4-}) concentration.

2.3. Process transfer to a 20-L bag-photobioreactor

A custom-built bag-photobioreactor (cBPB) as described in Supplement C was used for process transfer to a larger cultivation volume. Cells were grown in 10 L ESAW* at 21 °C, 350 µmol $m^{-2} s^{-1}$ irradiation, pH 8 and $pCO_{2,const}$ of 1% (0.1 vvm, headspace aeration). The culture was mixed at 60 ± 10 rpm. Concentrations of NO_3^- PO_4^{3-} and Ca^{2+} were measured daily and replenished by individual addition from their respective stock solutions, when necessary.

2.4. Offline analytics

Cell concentration in the culture broth was determined by flow cytometry (Guava EasyCyte 6-2L, Merck Millipore), with InCyte based on the FSC/RED2 signal. Device calibration was used to ensure that %CV for detection of particles per ml was < 5%. Specific growth rates were calculated by exponential regression over at least 4 data points within the culture exp-phase ($R^2 > 0.98$).

For the determination of coccolith concentration two different techniques were used. Manual counting using a Neubauer chamber was applied to shake flasks experiments and PBR samples with low estimated coccolith concentrations (< 0.5 g L^{-1},). The analysis required agglomerate-free solutions of coccoliths. In this regard, a 1.5 ml sample was pipetted into a micro reaction tube. The suspension was incubated at 80 °C for at least 48 h to facilitate cell disruption. The coccolith suspension was then diluted 10× with 5 g L^{-1} $NaHCO_3$. 1 ml of the diluted suspension was transferred to a fresh micro reaction tube and mixed with 6% NaOCl, shortly vortexed and incubated for 10 min. The mix was centrifuged for 6 min at 4 °C and 1.100 ∗*g* (Hettich, Mikro 220R). 1 ml supernatant was subsequently removed and discarded. The suspension was mixed with 1 ml 0.5 g L^{-1} $NaHCO_3$ and shortly vortexed. Centrifugation, supernatant removal and washing with 0.5*g* L^{-1} $NaHCO_3$ solution was repeated 3–5 times until a homogeneous solution without coccolith agglomerates was achieved. Coccolith concentration was then determined by using a Neubauer chamber ((Axio Scope A1, Infinity Analyze, Zeiss, 400× differential interference contrast) and counting coccolith numbers in at least 10 small squares. Coccolith concentration was then estimated according to Eq. (1). Average values and standard deviations were derived from technical triplicate measurements.

$$c_{coccoliths}\,[ml^{-1}] = \frac{n_{Coccoliths\ per\ small\ square}}{0.0025\,[mm^2] \bullet 0.1\,[mm]} \bullet 1000 \left[\frac{mm^3}{ml}\right] \quad (1)$$

To extrapolate mass concentration [g L^{-1}], absolute numbers were multiplied with specific coccolith weight, which was previously estimated to be 2.6 ± 0.23 pg $coccolith^{-1}$ (see Supplement D).

Coccolith concentration for dense samples (> 0.5 g L^{-1}) was measured gravimetrically (triplicate determination). Empty 2 ml micro reaction tubes were dried (48 h, 80 °C), cooled in a desiccator and subsequently weighed prior to sampling. Each tube was filled with 2 ml culture suspension and centrifuged for 10 min at 4 °C and 9670 ∗*g* (Hettich, Mikro 220R). Supernatant was discarded and pellet was suspended with 1.5 mL 0.5 g L^{-1} $NaHCO_3$ solution and incubated for 24 h at 80 °C. The following washing procedure was repeated 4–6 times until no cell-debris or coccolith agglomerates were visible under the microscope: centrifugation for 6 min at 220 ∗*g*, removal of supernatant and washing with 1.5 ml 0.5 g L^{-1} $NaHCO_3$. The pellet was then centrifuged one last time for 10 min at 9670 ∗*g* (Hettich, Mikro 220R), the supernatant was discarded and the pellet was dried at 80 °C for at least 48 h. The pellet-containing tube was then cooled in a desiccator and weighed. Coccolith mass concentration was then calculated from the weight difference of the empty and the pellet-filled tube. Volumetric coccolith productivity $r_{P,V}$ was estimated from coccolith concentration according to Eq. (2). From these individual data points, averages and standard deviations were calculated.

$$r_{P,V}\,[g\ L^{-1}d^{-1}] = \frac{c_{Coccoliths1} - c_{Coccoliths2}}{(t_1 - t_2)} \quad (2)$$

$r_{P,V}$ *coccolith productivity per* $Lc_{Coccoliths1}$ *measured concentration of coccoliths at* $t_1c_{Coccoliths2}$ *measured concentration of coccoliths at* $t_2t_1 - t_2$ *time difference between two measurement points* (*usually one day*)

For some experiments, cellular productivity $r_{P,C}$ was roughly estimated according to Eq. (3). From these individual data points, averages and standard deviations were calculated.

$$r_{P,C}\,[h^{-1}] = \frac{c_{Coccoliths1} - c_{Coccoliths2}}{c_{Cells2}\,(t_1 - t_2)} \quad (3)$$

$r_{P,C}$ *av. cellular productivity*$c_{Coccoliths1}$ *measured concentration of coccoliths at* $t_1c_{Coccoliths2}$ *measured concentration of coccoliths at* t_2c_{Cells2} *measured concentration of cells at* $t_2t_1 - t_2$ *time difference between two measurement points*

For the measurement of TA and calculation of the carbonate system, 10 mL culture filtrate (0.4 µm) was gran-titrated with 0.05 M HCl (SI

Table 2
Growth and coccolith formation.

Culture (n = 3)	Spec. μ_{max}	$c_{cells,max}$	Final coccolith concentration	$r_{P,V}$	$r_{P,C}$
	[d^{-1}]	[mL^{-1}]	[$g\,L^{-1}$]	[$g\,L^{-1}\,d^{-1}$]	[h^{-1}]
ESAW (=control)	0.98 ± 0.01	$4.2{\cdot}10^6$ ± $0.2{\cdot}10^6$	0.12 ± 0.01	0.014 ± 0.01	1.0 ± 0.3
$+HCO_3^-$	1.09 ± 0.08	$6.1{\cdot}10^6$ ± $0.3{\cdot}10^6$	0.38 ± 0.05	0.09 ± 0.06	–
$+HCO_3^-$, NO_3^-, PO_4^{3-}	1.11 ± 0.04	$1.4{\cdot}10^7$ ± $0.08{\cdot}10^7$	0.99 ± 0.01	0.12 ± 0.03	2.9 ± 1.3
$+HCO_3^-$, NO_3^-, PO_4^{3-}, Ca^{2+}	1.12 ± 0.07	$1.7{\cdot}10^7$ ± $0.08{\cdot}10^7$	1.51 ± 0.04	0.20 ± 0.09	2.8 ± 0.5
$+HCO_3^-$, NO_3^-, PO_4^{3-}, Ca^{2+}(2×)	1.02 ± 0.01		1.28 ± 0.11	0.18 ± 0.1	–
$+HCO_3^-$, NO_3^-, PO_4^{3-}, Ca^{2+}(0.1×)	1.08 ± 0.06	$1.4{\cdot}10^7$ ± $0.1{\cdot}10^7$	1.28 ± 0.10	0.18 ± 0.1	–

Analytics Titroline 7000). Due to the high sample volume, no measurement replication was performed. Samples grown at atmospheric pCO_2 were not diluted. Samples equilibrated at higher pCO_2 were diluted 1:10 with deionized water ($R > 14\,M\Omega$). TA is linear to the amount of protons necessary to neutralize the bases and can be calculated from titration data according to Dickson [67]. The calculation of the carbonate system components (DIC, $dHCO_3^-$, dCO_2, Ω) was performed using CO_2SYS [68]. Input values for the calculation were measured pH (online pH for PBR experiments), TA, temperature, salinity and phosphate concentration. Salinity was measured with a conductivity- and salinity measuring cell (TetraCon 325, WTW). Dissociation constants for carbonic acid obtained by Mehrbach, Dickson and Millero [69,70] were used for the calculation. Dissociation constants for sulfuric acid were those obtained by Dickson [71].

The concentrations of NO_3^- PO_4^{3-}, and Ca^{2+} were determined by using photometric assays (Spectroquant, Merck Millipore: NO_3^-:1.14941.0001/500 nm; PO_4^{3-}:1.14848.0002/880 nm, Ca^{2+}: 1.4815.0001/520 nm). The protocol from the manufacturer was adjusted for a 5-fold reduction in sample and chemical volumes. Samples were filtered (0.4 µm) and diluted with ultrapure water when necessary. Absorbance was determined in 1.5 mL polystyrene cuvettes. Due to its high sample volume requirement, absorbance measurements was performed without replicates. Substrate uptake rates r_X were calculated according to Eq. (4)

$$r_X\ [pg\ cell^{-1}d^{-1}] = \frac{c_{X1} - c_{X2}}{c_{cells}(t_1 - t_2)} \quad (4)$$

r_x *cellular uptake rate of substrate* Xc_{X1} *concentration of substrate X at* t_1c_{X2} *concentration of substrate X at* t_2c_{cells} *cell concentration at* t_2t_1 – t_2 *time difference between two measurement points* (*usually one day*)

3. Results and discussion

3.1. Shake flask cultivations

Preliminary experiments were conducted to obtain first insights into the impact of nutrient- and DIC availability on growth and coccolith production. The data was the basis for the subsequent medium adjustment in the PBR experiments.

3.1.1. Nutrient replenishment experiments

Reference cultures grown in ESAW exhibited a short lag-phase of 1–2 days and thereupon grew exponentially with a specific growth rate of $0.98\,d^{-1}$ (see Table 2). Growth rate decelerated from day seven, when PO_4^{3-} was depleted (Fig. 2). The maximum cell concentration of $4.2{\cdot}10^6$ cells mL^{-1} was achieved on day ten, simultaneously with the depletion of NO_3^-. The cultures exihibited no stationary phase. Instead, cell concentration dropped immediately after reaching peak value. During the cultivation TA and pH rapidly decreased to minimum values of 200 µmol kg^{-1} and 7.6, respectively (Fig. 3). Consequently, the concentration of all dissolved inorganic carbon species dropped as well. At day four after inoculation $\Omega CaCO_3$ was < 1, supporting unfavorable conditions for $CaCO_3$ precipitation and thus coccolith formation. Therefore, average $r_{P,V}$ of $0.014\,g\,L^{-1}\,d^{-1}$ and final concentrations of $0.12\,g\,L^{-1}$ were expectably low. A rough estimate gave an average cellular productivity of approximately 1 coccolith per hour, which is approximately what can be expected under natural conditions. The cultivation conditions adversely impacted coccolith morphology and integrity. Coccoliths harvested at day six, when medium pH was < 7.6, were incomplete and disintegrated (see Supplement E for ESEM pictures).

The impact of constant dissolved inorganic carbon (DIC)- and N-, P- and Ca availability was examined in combination with daily substrate replenishment.

As shown in Table 2, replenishment of organic carbon ($+HCO_3^-$) alone resulted in a 10%, increase of specific μ_{max} to 1.09 and maximum cell concentration to $6.1{\cdot}10^6\,mL^{-1}$. The course of substrate uptake was also similar to the reference culture. Exponential growth stopped on day seven after PO_4^{3-} was exhausted. From day seven onward, growth rate decelerated, on day eleven NO_3^- was depleted. Similar to the control cultures (ESAW), no stationary phase was observed. In contrast to the control, however, Ca^{2+} continuously decreased, and was used for coccolith formation until it was completely depleted between day eleven and day twelve. Coccoliths were produced with an average $r_{P,V}$ of $0.09\,g\,L^{-1}\,d^{-1}$ and a maximum concentration of $0.38\,g\,L^{-1}$ was harvested on day twelve. Although the calculated deviations are large, an increase in average cellular coccolith productivity could also be noted at about 2.9 ± $1.3\,h^{-1}$. This clearly shows that the product increase is due to a combination of higher cell concentration and individual cell productivity. The coccoliths harvested during the late exponential growth phase (day six) were structurally intact and did not exhibit any malformation. Regulating the carbonate system and preventing it from drifting towards low pH therefore proved as a necessary condition to increase coccolith productivity and quality.

However, it must be noted that after day seven, when PO_4^{3-} was depleted, no more coccoliths were produced. Replenishment of HCO_3^- only mitigated the drop of pH over time so that it was constantly maintained ≥8. TA and DIC minima dropped under 200 µmol kg^{-1}. This was especially severe between day six and day ten, when cell concentration was at its highest values. From day seven, $\Omega CaCO_3$ was temporarily < 1. This explains why no more coccoliths were produced after day seven.

Cultures, which were replenished with inorganic carbon ($+HCO_3^-$) and also PO_4^{3-} and NO_3^- exhibited a 10% higher spec. μ_{max} of $1.1\,d^{-1}$ and a three-fold maximum cell concentration of $1.4{\cdot}10^7\,mL^{-1}$. Under these conditions, a stationary phase was again not achieved. A possible explanation is the depletion of another substrate. In this regard the limitation model (compare Fig. 1 in the introduction section) indicates the depletion of Sr^{2+} or a trace element. Cells produced coccoliths with an average $r_{P,V}$ of 0.12 ± $0.03\,g\,L^{-1}\,d^{-1}$ yielding a maximum coccolith concentration of $1\,g\,L^{-1}$. This value exceeds the highest reported coccolith concentration of $0.7\,g\,L^{-1}$ previously obtained by Takano et al. [26].

The additional replenishment of Ca^{2+} resulted in an increase in average $r_{P,V}$ to $0.20\,g\,L^{-1}\,d^{-1}$ and a 50% increase in final coccolith concentration to $1.51\,g\,L^{-1}$. As illustrated by Fig. 2, NO_3^-, PO_4^{3-} and

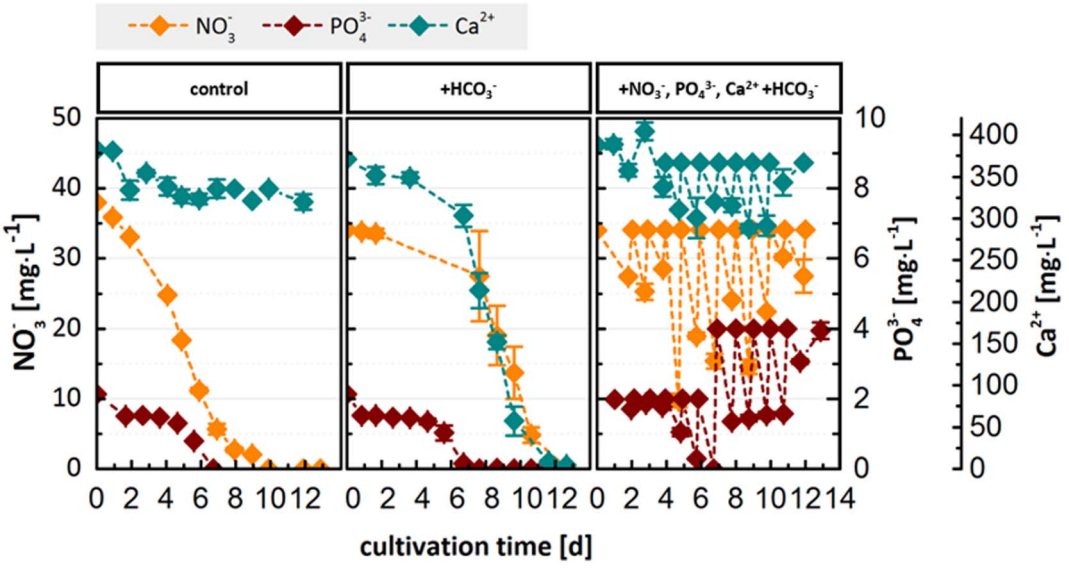

Fig. 2. Concentration profiles of NO_3^-, PO_4^{3-} and Ca^{2+} in the different setups. Control batch culture in ESAW (left). Cultures replenished with DIC ($NaHCO_3$) (middle). Cultures with replenishment of HCO_3^-, NO_3^-, PO_4^{3-} and Ca^{2+}. Error bars derive from biological triplicate determination (%CV < 5%).

Ca^{2+} were continuously taken up and PO_4^{3-} target values were raised to prevent limitation during the 24 h intermission between sampling. Interestingly, NO_3^- and PO_4^{3-} were still taken up, though to a much lesser extent, after day eleven. This means cells were taking up substrates although their concentration was already decreasing. Adjustment of Ca^{2+} target concentration (2-fold and 0.1-fold Ca^{2+}) did not have significant impact on growth. Instead both adjustments facilitated a 10% decrease of average $r_{P,V}$ to 0.18 g L^{-1} d^{-1} and a 20% reduction of final coccolith concentration to 1.28 g L^{-1}.

The results demonstrate that ESAW in its present form is not optimized for coccolithophorid mass cultivation and coccolith production. Despite being based on another strain, the stoichiometric limitation model shown in Fig. 1 agrees well with our observations. As predicted, N and P sources were consecutively depleted. ESAW thus restricts cell concentration to < 10^7 mL^{-1}. Replenishment of NO_3^-, PO_4^{3-}, Ca^{2+} did increase cell concentration but only to a limited extent.

3.1.2. *Experiments for optimizing initial substrate concentration*

The next logical step was to adjust the medium by elevating the initial concentrations of NO_3^-, PO_4^{3-}, Ca^{2+} and Sr^{2+} and trace elements without inducing growth inhibition. In this respect, cultivations were carried out in ESAW containing different initial concentrations of

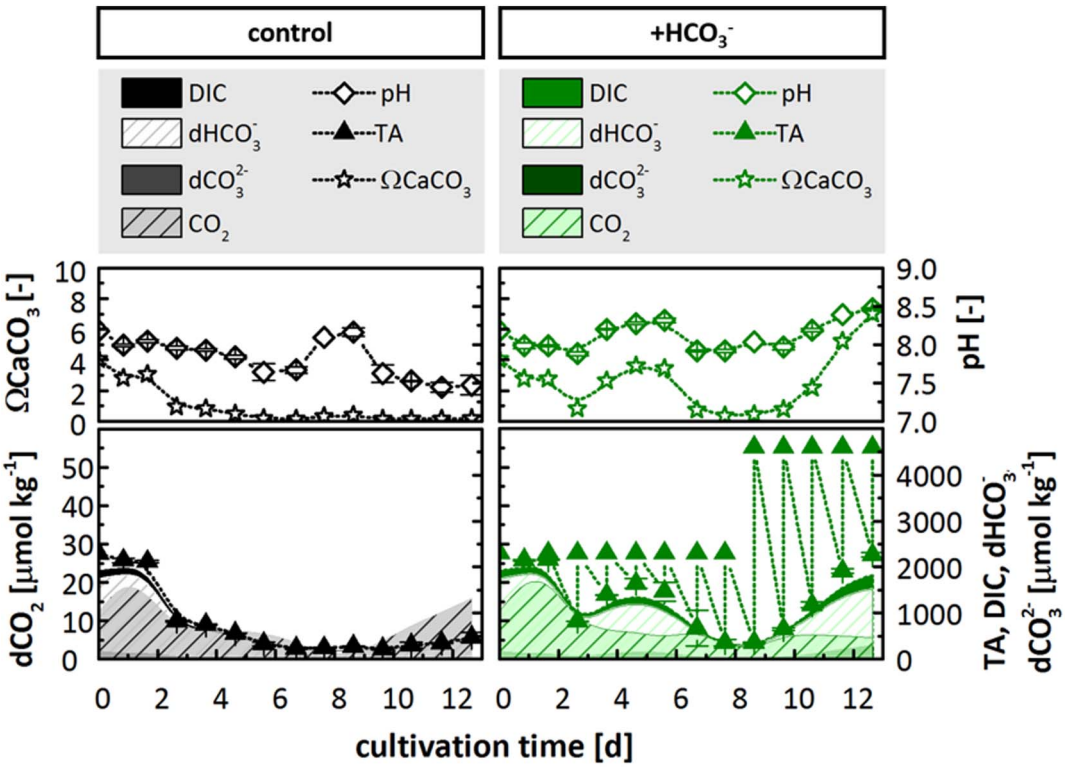

Fig. 3. Composition of the carbonate system of cultures grown in ESAW (left) and cultures daily replenished with DIC ($NaHCO_3$). Error bars derive from biological triplicate determination (%CV < 5%).

Table 3
Growth of *Emiliania huxleyi* RCC1216 by varying single substrate and combination of phosphate and nitrate concentrations. All experiments were performed in biological triplicates.

NO_3^-	μ_{max}	PO_4^{3-}	μ_{max}	NO_3^-	PO_4^{3-}	μ_{max}
[mg L^{-1}]	[h^{-1}]	[mg L^{-1}]	[h^{-1}]	[mg L^{-1}]	[mg L^{-1}]	[h^{-1}]
34.0	0.98 ± 0.01	2.0	0.98 ± 0.01	34.0	2.0	0.98 ± 0.01
170.0	1.01 ± 0.01	10.0	0.97 ± 0.01	170.0	10.0	0.91 ± 0.07
340.0	1.03 ± 0.03	20.0	1.06 ± 0.01	340.0	20.0	0.97 ± 0.03
1700.0	0.99 ± 0.01	100.0	Decrease in cell concentration	1700.0	100.0	Decrease in cell concentration
3400.0	0.95 ± 0.02	200.0	Decrease in cell concentration	3400.0	200.0	Decrease in cell concentration

Ca^{2+}	μ_{max}	Sr^{2+}	μ_{max}	Trace element stock solution	μ_{max}
[mg L^{-1}]	[h^{-1}]	[mg L^{-1}]	[h^{-1}]	[ml/L]	[h^{-1}]
66.0	0.98 ± 0.01	7.0	0.98 ± 0.01	1	0.98 ± 0.01
132.0	0.63 ± 0.15	14.0	0.90 ± 0.02	5	0.98 ± 0.03
330.0	Decrease in cell concentration	35.0	0.92 ± 0.01		
660.0	Decrease in cell concentration	70.0	0.77 ± 0.10		

NO_3^-, PO_4^{3-}, Ca^{2+}, Sr^{2+} and trace elements.

As evident from Table 3, raising initial NO_3^-, and PO_4^{3-} concentrations (100- and 25-fold, respectively) did not affect spec. μ_{max}. This was also the case when both substrates were simultaneously elevated. Initial Sr^{2+} concentrations up to 0.84 mM (10-fold) and 5-fold increase in trace element concentration also did not decrease growth rate. As expected, a 2-fold increase in initial $CaCl_2$ concentration already caused severe growth inhibition with $\mu_{max} = 0.63\,d^{-1}$ (−36%). Based on this information, an adapted version of ESAW (ESAW* see Supplement B) was introduced which contained the 25-fold initial concentrations of $NaNO_3$ and $NaH_2PO_4{\cdot}H_2O$ and 5-fold initial concentrations of Sr^{2+} and trace elements. $CaCl_2$ concententration must not be increased. Instead, it must be regularly replenished, or better, continuously delivered by automated feeding.

3.1.3. $CaCO_3$ as an alternative Ca^{2+} source

Because of the growth inhibition caused by dissolved Ca^{2+}, $CaCO_3$ was tested as a potential slow-release substrate. The idea was to use the low solubility of $CaCO_3$ (14 mg/L) to support a low concentration of dissolved Ca^{2+}, but at the same time maintaining an automatic equilibrium-driven replenishment. After medium preparation, solid, random sized (up to 10 µm), amorphous $CaCO_3$ particles were visible in the medium. These precipitates absorbed most of the light and the transmission at the beginning of the experiment was very low, between 0.5% (nm) and 1% (700 nm). The precipitates unfortunately prevented the determination of cell concentration by flow cytometry as they can clog the equipment's sensitive flow capillary. Manual counting was also not possible because cells and precipitates overlapped and could not be discriminated from each other. Due to the high $CaCO_3$ concentration, the photometric determination of Ca^{2+} could not be carried out at any time of the experiment. However, it can be assumed that $CaCO_3$ was dissolved continuously as long as precipitates were visible. In this case, the absolute amount of dissolved Ca^{2+} depended on the difference between $CaCO_3$ release rate and the Ca^{2+} uptake rate of the cells, which is hard to estimate.

During the cultivation, a proliferation of cells over time could be tracked qualitatively by microscopy. As the amount of precipitate slowly decreased over time, the culture suspension changed its color from white to green-yellow. This disappearance of $CaCO_3$ precipitates on day twelve made it possible to determine cell concentration ($6.3{\cdot}10^6 \pm 0.48{\cdot}10^6$ mL^{-1}). The cell concentration subsequently declined in the following days. Fig. 4 shows the composition of the carbonate system under these conditions. Total alkalinity in fresh medium was initially 3500 µmol kg^{-1} and did not decrease > 500 µmol kg^{-1} during cultivation. DIC and HCO_3^- decreased gradually until day twelve, but always remained above sea water concentrations (1800–2400 µmol kg^{-1}). This was probably due to the continuous dissolution of $CaCO_3$ as secondary effect of calcification. Compared to batch experiments containing $CaCl_2$ as Ca^{2+} source, the carbonate system remained exceptionally stable. Even though the presence of the $CaCO_3$ particles also made absolute coccolith quantification impossible, an increase in coccolith concentration was observed throughout the cultivation by microscopy. This suggests that it is possible to use solid $CaCO_3$ as Ca^{2+} substrate in principle. The stable carbonate system could be an advantage when no active regulation of carbonate chemistry is necessary. Moreover, the initial medium turbidity derived by $CaCO_3$ particles could prevent cultures from light inhibition in outdoor cultivations. Nevertheless, a lower $CaCO_3$ concentration which causes higher initial light transmission and supports faster growth should be chosen.

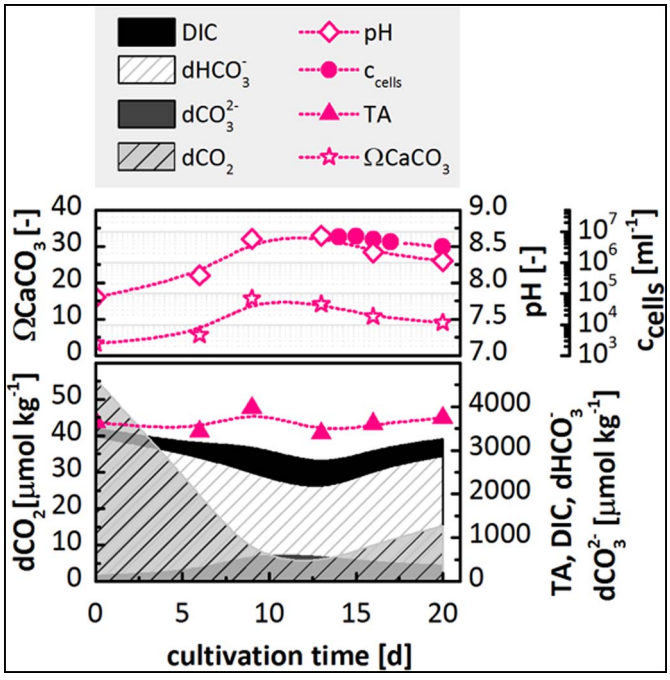

Fig. 4. Cell concentration and carbonate system chemistry in cultures with $CaCO_3$ as main Ca and DIC source.

3.2. Experiments in photobioreactors under controlled conditions

The production of coccolith was further investigated in a 2-L stirred tank photobioreactor (PBR). From the shake flask cultivations it became clear, that manual addition of $NaHCO_3$ offers an option to regulate the carbonate system to some extent. However, this technique is laborious and not suitable to provide a stable long-term carbonate system.

In the PBR, carbonate system was therefore adjusted by controlling pH and pCO_2 directly. Two fundamentally different carbonate system setpoints were examined. The first setpoint (pH 8.2, dissolved $pCO_{2,const}$ = 0.04–0.06%) supported a low carbon scenario, which is closer to the conditions in the ocean or a shake flask [49]. The second one (pH 8, dissolved $pCO_{2,const}$ = 1%) supported a high carbon scenario delivering an excess supply of all carbon species, and a slight equilibrium shift towards CO_2.

3.2.1. Low carbon conditions ($pCO_{2,const}$ = 0,04–0,06%, pH = 8.2)

In the first experiment, cells were cultured in ESAW and no substrates were replenished. The growth profile clearly differed from that of the equivalent shake flask experiment (compare Fig. 5). After a two day lag phase, cells grew exponentially with a 40% lower specific μ_{max} of 0.62 d^{-1}. On day eight, after reaching a maximum cell concentration of $8{\cdot}10^5$ mL^{-1}, the exponential growth phase was immediately followed by a reduction in cell concentration. Setpoint values for low carbon conditions, especially pH, were slightly overdriven in the first two days of cultivation (Fig. 6). However, DIC and all corresponding carbonate species were always available in sufficient amounts. From day two the setpoint values for dissolved pCO_2 and pH remained within their permitted deviation (< 5%). Carbonate system was constant between day two and day six (DIC = 7500 µmol kg^{-1}, HCO_3^- = 7000 µmol kg^{-1}, CO_2 = 4–5 µmol kg^{-1}). The concentration of DIC and HCO_3^- dropped to approximately 5000 µmol kg^{-1} and 4800 µmol kg^{-1}, respectively, by day twelve. The concentration of CO_2, however, remained constant throughout the cultivation. Producing coccoliths in original ESAW, analogous to the shake flask control cultures, resulted in expectably limited success and only 0.22 g L^{-1} coccoliths were harvested.

When NO_3^-, PO_4^{3-} and Ca^{2+} were replenished daily, cells grew even slower with a specific μ_{max} to 0.5 d^{-1}. This was only 50% of specific μ_{max} observed in the analogous shake flask experiments and approximately 40% of the μ_{max} this strain is able to grow at best [61]. An explanation for this could be that Ca^{2+} availability channeled more carbon into the formation of coccoliths under low carbon conditions. As a result of slower growth, exponential growth phase was extended until day 17, reaching a maximum cell concentration of $6.7{\cdot}10^5$ mL^{-1}. Again, cell concentration decreased immediately thereafter. The conditions allowed an active culture to last almost a week longer than in the shake flask cultures. Despite slower growth, the coccolith concentration was drastically increased. Cells produced coccoliths throughout the cultivation with an average $r_{P,V}$ = 0.22 g L^{-1} d^{-1}, resulting in a final concentration of ca 3.5 g L^{-1} This was twice the amount harvested from the analogous shake flask experiment. However, average cellular productivity $r_{P,C}$ was reduced compared to the corresponding shake flask experiments. That means that the cells were individually less productive and this was compensated for the high final concentration with the length of the production phase.

3.2.2. High carbon conditions

Further experiments were conducted in a 2-L PBR under high carbon conditions (pCO_2 = 1%, pH = 8). In a first attempt, a culture was replenished with NO_3^-, PO_4^{3-} and Ca^{2+}. The dissolved pCO_2 was not controlled, instead the culture liquid was constantly aerated with 1% CO_2 ($pCO_{2,inital}$ = 1%). Cells grew exponentially from day two with μ_{max} = 0.75 d^{-1} until day nine, reaching a maximum cell concentration of $3.1{\cdot}10^7$ mL^{-1} (Fig. 7). Cell concentration decreased immediately after reaching this peak value. Coccoliths were produced with an average r_P of 0.14 g L^{-1} d^{-1}. However, it was observed that the actual rate slowed down over time and a final concentration of 0.94 g L^{-1} was harvested on day eleven. Although growth performance was improved, $r_{P,V}$ was comparably slow. The most obvious reason was the drifting carbonate system. Since pCO_2 was not controlled, it continuously decreased from the initial 1% to 0.15% on day nine. Consequently, the carbonate system was not stable during the cultivation and the concentration of all carbonate system components dropped (Fig. 8). The rate of DIC uptake by the growing and calcifying cells was logically much faster than the CO_2 transfer rate. Aeration with 1% CO_2 was therefore not suitable for the maintenance of a steady carbonate system under process conditions. One reason is probably the slenderness ratio of the used PBR, which was suboptimal for gas transfer through headspace aeration. A better mass transfer supported by a greater area-to-volume ratio and also higher flow rates can certainly mitigate this effect. However, aeration with CO_2 and solely controlling pH can be a compromise when no dissolved pCO_2 control unit is available and the focus is exclusively on coccolith production. An alternative could be to use offline titration data and manually increase the concentration of CO_2 in the influent gas when necessary. In any case, studies on physiological responses to carbonate chemistry should be conducted under constant carbonate system control provided by simultaneous pH/dissolved pCO_2 control or by continuous cultivation.

The difference between sole CO_2 aeration and pCO_2 control was demonstrated in the following experiment. Additionally, modified ESAW* (see Supplement B) was used in this cultivation, which contained higher initial concentrations of NO_3^-, PO_4^{3-}, Ca^{2+}, Sr^{2+} and trace elements. To maintain a constant pCO_2, the controller mixed incoming gas (air) with up to 5% CO_2 to compensate DIC consumption during cultivation. pCO_2 and pH were constant within their allowed deviation (± 5%). Cells grew exponentially from day two with specific μ_{max} = 0.71 d^{-1}. Growth rate reduced during day nine and cell number slightly fluctuated around $2.9{\cdot}10^7$ mL^{-1} for 12 days until day 21. At this concentration, the medium was completely opaque white and glittering (Fig. 9). This was the first time a culture of *E. huxleyi* exhibited a

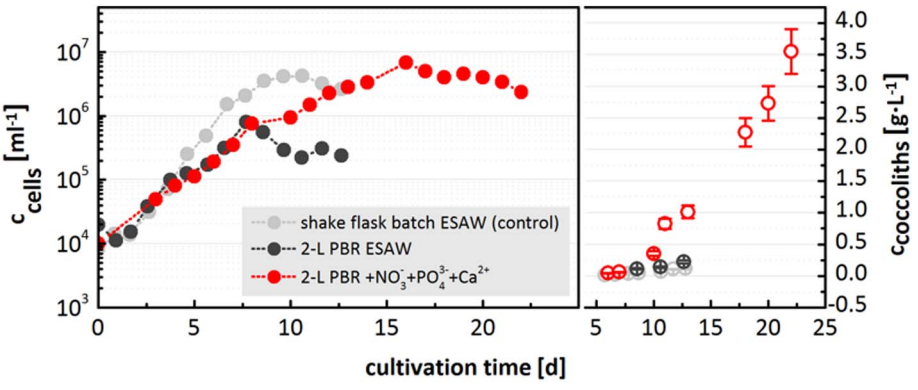

Fig. 5. Cell– and coccolith concentrations of *E. huxleyi* RCC1216 during cultivation in a 2-L stirred PBR under low carbon conditions (pCO_2 = 0.04–0.06%, pH = 8.2). Coccolith concentration was determined in measurement triplicates (%CV < 5%).

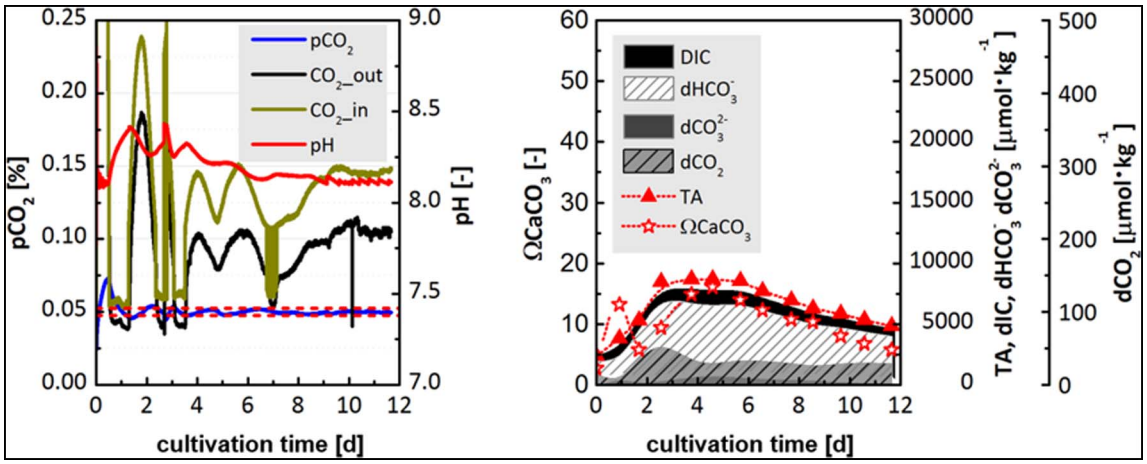

Fig. 6. Online measurement of pH and pCO_2 under low carbon conditions ($pCO_{2,const}$ = 0.04–0.06%, pH = 8.2) (left) and resulting carbonate system chemistry (right).

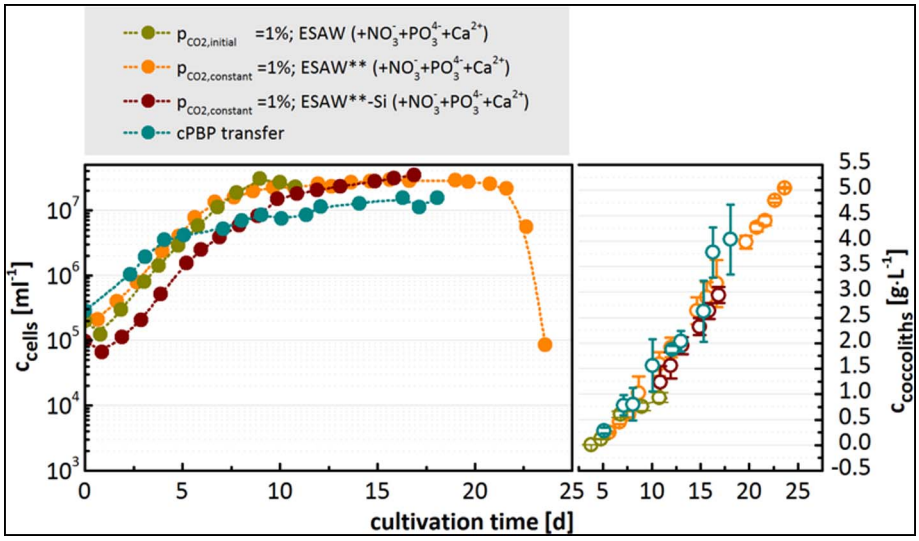

Fig. 7. Cell- and coccolith concentrations of *E. huxleyi* RCC1216 during cultivation in a 2-L stirred PBR and a custom-build bag-photobioreactor (cBPB) under high carbon conditions (pCO_2 = 1%, pH = 8). Coccolith concentration was determined in measurement triplicates (%CV < 5%).

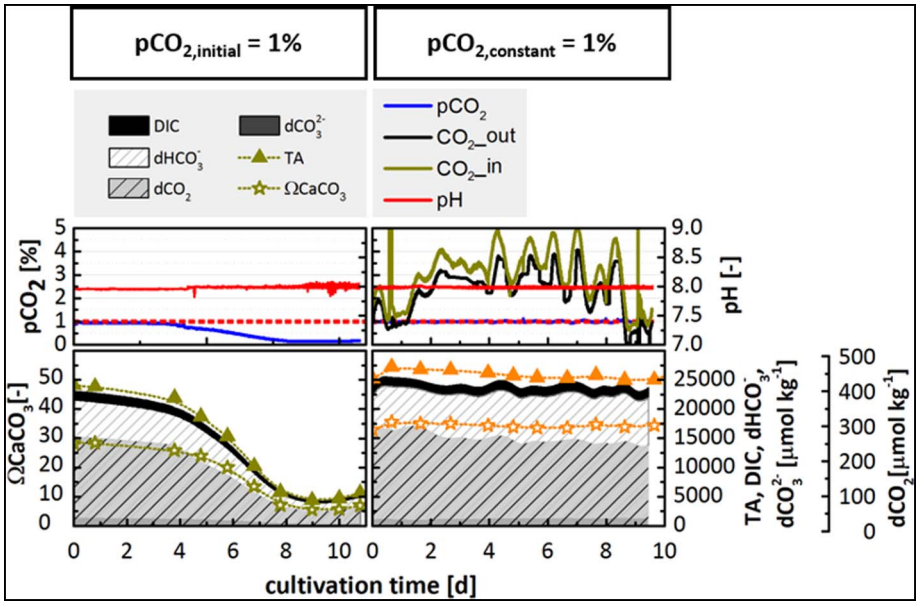

Fig. 8. Online measurement of pH and pCO_2 under high carbon conditions) and resulting carbonate system chemistry. (Left) $pCO_{2,initial}$ = 1%, pH = 8.2. (Right) $pCO_{2,const}$ = 1%, pH = 8.2.

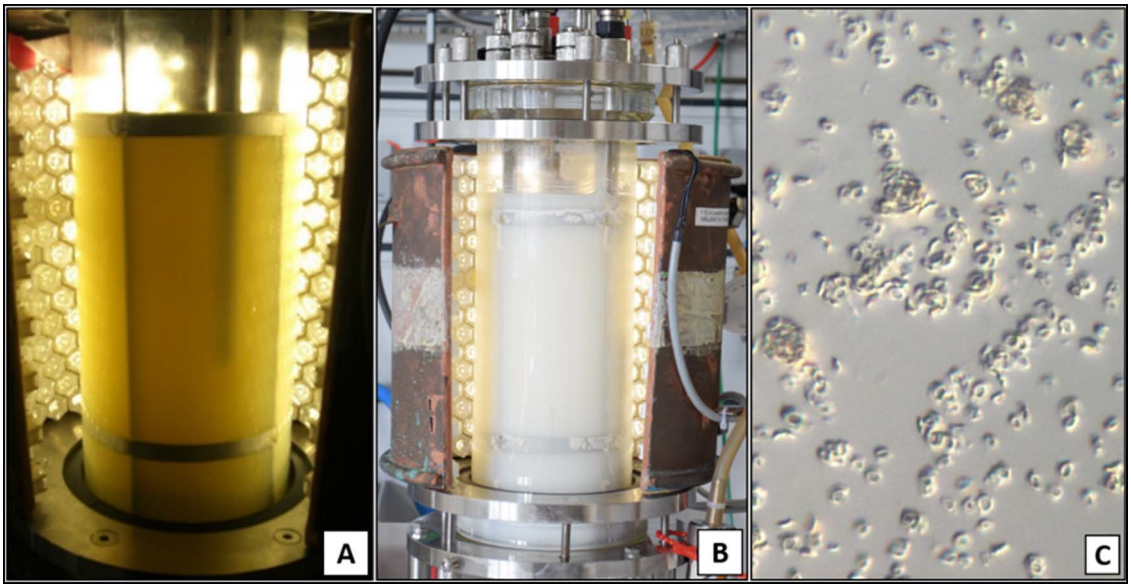

Fig. 9. Picture of the culture suspension during cultivation in a 2-L stirred PBR at $pCO_{2,constant}$ = 1%, ESAW* (+NO_3^-, PO_4^{3-} and Ca^{2+}). (A) Yellow culture suspension during late exponential phase (d6). (B) Culture at day 17. With increasing production of coccoliths the medium turned completely white and opaque. (C) Light Microscopy picture of culture suspension at 5 g L^{-1} (d23) (400×, DIC, Zeiss Axio Scope A1). (For interpretation of the references to color in this figure legend, the reader is referred to the web version of this article.)

stationary phase at such a high cell concentration over a long period of time. After day 21 the cell concentration decreased and the cultivation was terminated by adjusting irradiance to 2000 µmol m^{-2} s^{-1}. Interestingly, cells rapidly degraded and no cells were counted after 72 h. The irradiance which terminated the process resembles an average sunny day in middle Europe. Although this could be challenging in outdoor production, the observed effect could also be exploited for coccolith separation or purification. Exposure to sunlight could for example replace the energy-intensive heat induced cell disruption.

Coccoliths were produced during the entire cultivation with $r_{P,V}$ = 0.27 g L^{-1} d^{-1} and 5.1 g L^{-1} were harvested on day 23. ESEM Analysis showed that these coccoliths were homogeneous and intact (see Supplement E). Despite these high final concentrations, the average cell performance was drastically reduced ($r_{P,C}$ = 0.2 ± 0.05 h^{-1}). It seems that with increasing cell- and coccolith density, cellular productivity decreases. This also becomes evident when looking at the course of productivity over time (data not shown). Cellular productivity decreased over time and became stable on a comparably low level during stationary phase. This suggests that the decline in productivity and also growth rate may have resulted from poor light supply, which became stronger as the cell and product concentrations increased. It must be taken into account that titration with NaOH supported an increase in salinity over time, which was approximately proportional to the amount of formed coccoliths. In the case of producing 5.1 g L^{-1} coccoliths under high carbon conditions, the salinity rose from approximately 30 ppt to 35 ppt. It is known that salinity tolerance is limited in most phytoplankton and also in *E. huxleyi* [72]. A third factor could be shear stress, which was introduced by the stirring motion. However, in order to be able to make more precise statements, further tests including more extensive sampling must be carried out in the future. The high volumetric productivity, in this case, clearly demonstrates how the number of cells can compensate for their individual loss of productivity.

Although initial substrates for NO_3^- and PO_4^{3-} were increased 25-fold in ESAW*, replenishment of these substrates was necessary on day twelve (PO_4^{3-}) and day 20 (NO_3^- and PO_4^{3-}). For both of these substrates, uptake rates exponentially decreased during the exponential phase of cultivation (first 5–7 days) and subsequently fluctuated around 1–5 pg $cell^{-1}$ d^{-1} from day ten during linear- and stationary phase (Fig. 10). This phenomenon was also observed in shake flask cultivations (data not shown). This is probably due to storage of phosphate and nitrogen during excess conditions, which is a common phenomenon in green- and red microalgae [73–75]. Although similar mechanisms are yet to be reported for *E. huxleyi*, there are modeling studies indicating their existence [76]. An interesting approach could be to feed limited amounts of PO_4^{3-} and NO_3^-, supplying only enough substrate for growth but prevent the formation of storage compounds. This so-called microfeeding may allow to channel more energy into growth and calcification and therefore further increase coccolith productivity and final concentrations. Microfeeding would also be a suitable option to deliver Ca^{2+} without substrate inhibition. The most reasonable solution is the adjustment of feeding rate to the cellular Ca^{2+} uptake rates, which was comparably constant (10 ± 2 pg cell d^{-1}) during the cultivation.

Calcification is shown to be dependent on the availability of nutrients in the medium, since the process immediately stopped upon PO_4^{3-} depletion. The limitation model (Fig. 1) gave an excellent prognosis about the order of substrate depletion. Increasing the concentration of Sr and trace elements in ESAW* supported a long-term stationary phase with actively coccolith producing cells. This resulted in extraordinarily high coccolith concentrations > 5 g L^{-1}. Unfortunately, there was no analytical method available to determine Sr or trace metal concentration during the experiments. For further medium optimization, Sr and trace metal uptake should be examined.

To summarize, it can be said that the choice of carbonate system setpoints did not influence coccolith productivity significantly. It was demonstrated that combined pH/dissolved pCO_2 control was reliable in both cases and facilitated to maintain all dissolved carbonate species in the same absolute and relative concentration throughout the cultivation. Additionally the coccoliths, which were harvested from cultivation under low and under high carbon conditions did not exhibit any obvious differences (see Supplement E). It is therefore comprehensible, that the absolute concentrations of dissolved CO_2, HCO_3^- and CO_3^{2-} and their ratio are not even important for coccolith production, as long as there is enough HCO_3^- and as long pH is not far under 8. These findings are in agreement with Bach et al., who studied the impact of carbonate chemistry in dilute batch cultures [45]. They found that neither growth nor calcification is sensitive to low CO_2 and low HCO_3^- as well to pH beyond a limited range, but not to elevated CO_2 and HCO_3^-. Our results suggest that this is also true for coccolithophorid mass cultivation.

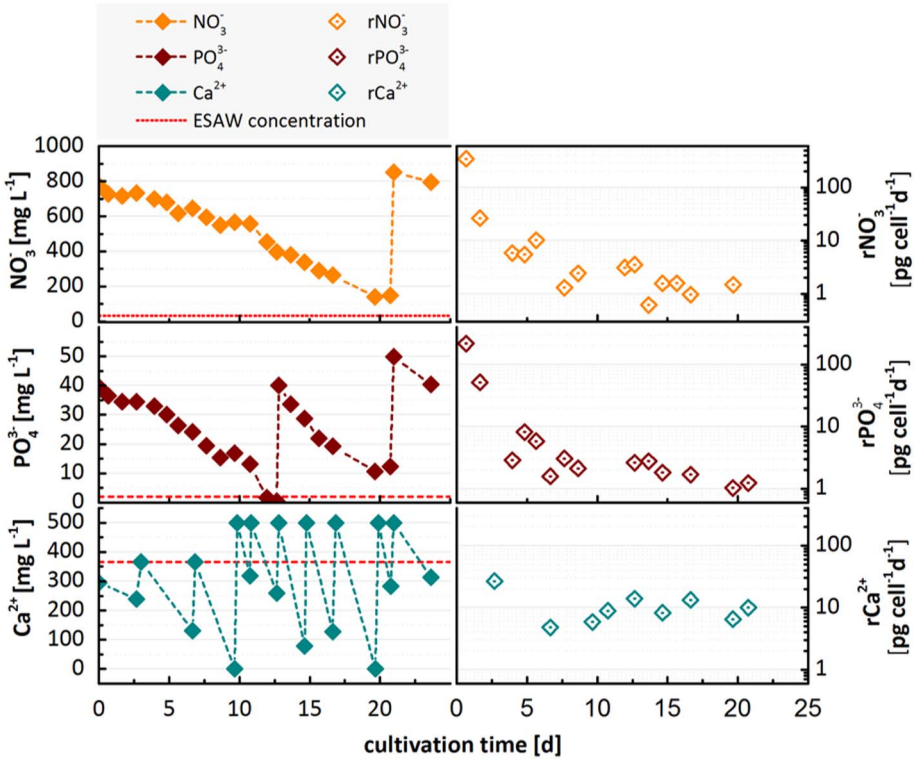

Fig. 10. Measured concentrations of substrates NO_3^-, PO_4^{3-} and Ca^{2+} (left) and derived substrate uptake rates (right) during cultivation of *E. huxleyi* RCC1216 in ESAW* under high carbon conditions (pCO_2 = 1%, pH = 8).

3.2.3. Reduction of silicon concentration

During evaluation of the experiments, we observed the formation of magnesium silicate particles (data not shown). These were interfering with particle analyzes and had to be removed from the coccolith suspension with additional washing steps. Therefore, we reduced silicon concentration in the medium (0.97 mg L^{-1} SiO_4^{4-} corresponds to a 90% reduction) to minimize the precipitation of magnesium silicate. The reduction of $Na_2SiO_3 * 5H_2O$ (ESAW*-Si) did not impede initial cell growth. Cells grew exponentially with specific μ_{max} of 0.74 d^{-1} and a maximum cell concentration of $3.4 \cdot 10^7$ mL^{-1} was obtained on day nine. Although coccoliths were produced with satisfactory production rates of $r_{P,V}$ of 0.28 g L^{-1} d^{-1} (compare Table 4 and Fig. 7), they were malformed and brittle-looking (see Supplement E). Thus, when intact coccoliths are to be produced, it is not recommended to reduce the silicon concentration drastically. We previously demonstrated that Si is included in the coccolith material [4]. Previous studies have shown that Si- uptake inhibitors and Si depletion in late stages of cultivation do not adversely affect *E. huxleyi's* growth and coccolith morphology [77]. This is in contradiction to our results and could be explained by genetic differences between the strains used. While Durak et al. used the Norwegian strain *E. huxleyi* Ply-B92/11 in their study, our experiments were conducted with a strain isolated from the Pacific Ocean. Strains of *E. huxleyi* can express extensive genetic variation [28] and behave very differently, for example expressing different pigment composition and morphotypes [78,79].

3.2.4. Process transfer to a 20-L customized bag-photobioreactor

Process conditions were finally transferred to a 20-L custom-made bag-photobioreactor (cBPB) (see Supplement C). Cells were cultured for 18 days in total. The exponential growth phase was shorter than in the stirred PBR with μ_{max} = 0.62 d^{-1} for four days. Cells decreased their growth rate from day five but continued growing to obtain a maximum cell concentration of $1.6 \cdot 10^7$ mL^{-1}. Coccoliths were produced with an average $r_{P,V}$ of 0.32 g L^{-1} d^{-1}, which was the highest coccolith production rate in all performed experiments and ever reported in literature. After termination of the experiment, a maximum concentration of 3.8 g L^{-1} coccoliths was harvested. ESEM analyzes showed that these coccoliths exhibited no malformations (see Supplement E). This means, that process transfer delivered almost 40 g of intact coccoliths in one batch for the first time.

Although all necessary nutrients were available in the beginning of the cultivations in the PBR and the cBPB, maximum specific growth rates were approximately 60–70% smaller in the stirred PBR and 55% smaller in the cPBP than in shake flask cultivations. A shear-stress induced decrease was probably a part of the explanation but certainly not the key factor. The gentle waving-motion of the cBPB caused less shear stress than the two rushton turbines in the stirred tank reactor. Still, maximum specific growth rate was slower in the cBPB. A second factor impeding growth rate was most likely light availability. All cultures were illuminated with the same photon flux density of 350 µmol m^{-2} 2^{-1}, but every cultivation system had a different layer thickness and therefore different illuminated area to volume ratio (see Table 5). A/Vs were approximately 26% smaller in the stirred PBR and 57% smaller in the cBPB. This means, there were larger light-limited zones in these systems, caused by coccolith light absorption and mutual shading of the cells. Another important factor influencing statistical light limitation is the trajectory of individual cells through the reactor. Since the cBPB provided a more gentle mixing, it is conceivable for a cell travelling through the culture medium to spend more time in light-limited zones. This issue becomes more severe, when high concentrations of coccoliths are present, which drastically reduce the light path. Layer thickness and light availability should definitely be considered in the optimization of reactor geometry.

4. Conclusion

In this article, we present the successful development of a batch process suitable for the production of coccoliths in the g L^{-1} scale. The basic pillars of this process were (1) a cultivation environment supporting light supply and bubble-free homogenization and aeration (2) a control of the carbonate system, which reliably enabled a pH ≥ 8, and the constant subsequent delivery of DIC, and (3) the constant supply with PO_4^{3-}, NO_3^-, Ca^{2+} and Sr^{2+} in non-inhibiting concentrations.

We hope to provide a starting point for further developments and to increase the interest in coccolithophorid mass cultivation. In order to face the increasing demand for coccoliths for application development,

Table 4
Growth and Coccolith formation.

Culture (n = 1)	spec. μ_{max}	$c_{cells,max}$	Final coccolith concentration	$r_{P,V}$	$r_{P,C}$
	[d^{-1}]	[mL^{-1}]	[$g\,L^{-1}$]	[$g\,L^{-1}\,d^{-1}$]	[d^{-1}]
Low carbon scenario					
2-L PBR ESAW	0.62	$8.0{\cdot}10^5$	0.22	0.03	–
2-L PBR + NO_3^- + PO_4^{3-} + Ca^{2+}	0.50	$6.7{\cdot}10^6$	3.55	0.22	0.6 ± 0.4
High carbon scenario					
$pCO_{2,initial}$ = 1%; ESAW (+NO_3^- + PO_4^{3-} + Ca^{2+})	0.75	$3.1{\cdot}10^7$	0.94	0.14	–
$pCO_{2,constant}$ = 1%; ESAW* (+NO_3^- + PO_4^{3-} + Ca^{2+})	0.71	$2.9{\cdot}10^7$	5.1	0.27	0.2 ± 0.05
$pCO_{2,constant}$ = 1%; ESAW*-Si (+NO_3^- + PO_4^{3-} + Ca^{2+})	0.74	$3.4{\cdot}10^7$	2.9	0.28	–
cPBP transfer	0.62	$1.6{\cdot}10^7$	3.8	0.32	0.5 ± 0.15

Table 5
light availability in different cultivation systems.

	Illumination	Layer thickness d	Illuminated area A	A/V
		[cm]	[cm^2]	[m^{-1}]
Shake flask	LED-panel below	3	88	44
Stirred PBR	Cylindrical LED coat covers 2/3 of culture volume	4,15	520	33
cBPB	LED sky	5,24	1900	19

the main challenge will be to transfer coccolith production to large-scale systems and to find better alternatives that take into consideration reactor geometry and process mode. Another important aspect will be the automatization of substrate feeding, which will make it possible to carry out the production of coccoliths with significantly less effort. When these challenges are mastered, *Emiliania huxleyi* has a realistic chance of joining the ranks of production organisms in the future.

Supplementary data to this article can be found online at https://doi.org/10.1016/j.algal.2018.01.013.

Acknowledgments

The underlying research project is funded by The German Federal Ministry of Education and Research (BMBF) within the bioeconomy 2020 program [grant number 031A158A]. We would especially like to acknowledge Lucas Marmin, who was involved in the development of the cBPB system and process transfer.

Declaration of authors contribution

We declare, that all Authors listed on the title page have contributed significantly to the work. All authors agree that the author list is correct in its content and order.

Study conception and design: Jakob.
Acquisition of data: Jakob, Weggenmann.
Analysis and interpretation of data: Jakob, Weggenmann, Posten.
Drafting of manuscript: Jakob, Posten.
Critical revision: Jakob, Posten.

Statement of informed consent, human/animal rights

No conflicts, informed consent, human or animal rights applicable.

Declaration of authors agreement to authorship and submission

We declare that all authors have seen and approved the manuscript being submitted for publication in Algal research. We warrant that the article is the Author's original work. We warrant that the article has not received prior publication and is not under consideration for publication elsewhere. On behalf of all Co-Authors, the corresponding Author shall bear full responsibility for the submission.

Conflict of interests

The authors declare that they have no competing interests.

References

[1] A. Sahni, Biomineralization: some complex crystallite-oriented skeletal structures, J. Biosci. 38 (2013) 925–935.
[2] J.R. Young, S.A. Davis, P.R. Brown, S. Mann, Coccolith ultrastructure and biomineralisation, J. Struct. Biol. 126 (1999) 195–215.
[3] J.M. Didymus, J.R. Young, S. Mann, Construction and morphogenesis of the chiral ultrastructure of coccoliths from the marine alga *Emiliania huxleyi*, P. Roy. Soc. B-Biol. Sci. 258 (1994) 237–245.
[4] I. Jakob, M.A. Chairopoulou, M. Vučak, C. Posten, U. Teipel, Biogenic calcite particles from microalgae - Coccoliths as a potential raw material, Eng. Life Sci. 45 (2017) 158.
[5] L. Addadi, A. Gal, D. Faivre, A. Scheffel, S. Weiner, Control of biogenic nanocrystal formation in biomineralization, Isr. J. Chem. 56 (2016) 227–241.
[6] A. Gal, R. Wirth, Z. Barkay, N. Eliaz, A. Scheffel, D. Faivre, Templated and self-limiting calcite formation directed by coccolith organic macromolecules, Chem. Commun. 53 (2017) 7740–7743.
[7] H.R. Thierstein, J.R. Young, Coccolithophores, first ed., Springer Berlin Heidelberg, Berlin, Heidelberg, 2004.
[8] B.A. Read, J. Kegel, M.J. Klute, A. Kuo, S.C. Lefebvre, F. Maumus, C. Mayer, J. Miller, A. Monier, A. Salamov, J. Young, M. Aguilar, J.-M. Claverie, S. Frickenhaus, K. Gonzalez, E.K. Herman, Y.-C. Lin, J. Napier, H. Ogata, A.F. Sarno, J. Shmutz, D. Schroeder, C. de Vargas, F. Verret, P. von Dassow, K. Valentin, Y. Van de Peer, G. Wheeler, J.B. Dacks, C.F. Delwiche, S.T. Dyhrman, G. Glöckner, U. John, T. Richards, A.Z. Worden, X. Zhang, I.V. Grigoriev, Pan genome of the phytoplankton *Emiliania* underpins its global distribution, Nature 499 (2013) 209–213.
[9] A.J. Poulton, T.R. Adey, W.M. Balch, P.M. Holligan, Relating coccolithophore calcification rates to phytoplankton community dynamics: regional differences and implications for carbon export, Deep-Sea Res. Pt. II 54 (2007) 538–557.
[10] W.M. Balch, K. Kilpatrick, P.M. Holligan, T. Cucci, Coccolith production and detachment by *Emiliania huxleyi* (Prymnesiophyceae), J. Phycol. 29 (1993) 556–575.
[11] P. Westbroek, Calcification in Coccolihophoridae – wasteful or functional (*Emiliania huxleyi*)? Environmental biogeochemistry, Proc. 5th International Symposium Stockholm, 1983, pp. 291–299.
[12] J.A. Raven, K. Crawfurt, Environmental controls on coccolithophore calcification, Mar. Ecol. Prog. Ser. 470 (2012) 137–166.
[13] B.N. Jaya, R. Hoffmann, C. Kirchlechner, G. Dehm, C. Scheu, G. Langer, Coccospheres confer mechanical protection: new evidence for an old hypothesis, Acta Biomater. 42 (2016) 258–264.
[14] K. Kayano, Y. Shiraiwa, Physiological regulation of coccolith polysaccharide production by phosphate availability in the coccolithophorid *Emiliania huxleyi*, Plant Cell Physiol. 50 (2009) 1522–1531.
[15] M. Marsh, Regulation of $CaCO_3$ formation in coccolithophores, Comp. Biochem. Physiol. B 136 (2003) 743–754.
[16] C. Brownlee, G.L. Wheeler, A.R. Taylor, Coccolithophore biomineralization: new questions, new answers, Semin. Cell Dev. Biol. 46 (2015) 11–16.
[17] T. Hassenkam, A. Johnsson, K. Bechgaard, S.L. Stipp, Tracking single coccolith dissolution with picogram resolution and implications for CO_2 sequestration and ocean acidification, P. Natl. Acad. Sci. USA 108 (2011) 8571–8576.
[18] M. Iwasaka, Y. Mizukawa, Magneto-optical properties of biogenic photonic crystals

in algae, J. Appl. Phys. 115 (2014) 17B501.
[19] Y. Mizukawa, Y. Miyashita, M. Satoh, Y. Shiraiwa, M. Iwasaka, Light intensity modulation by coccoliths of *Emiliania huxleyi* as a micro-photo-regulator, Sci. Rep. UK 5 (2015) 13577.
[20] N.R. Moheimani, J.P. Webb, M.A. Borowitzka, Bioremediation and other potential applications of coccolithophorid algae: a review, Algal Res. 1 (2012) 120–133.
[21] A.W. Skeffington, A. Scheffel, Exploiting algal mineralization for nanotechnology: bringing coccoliths to the fore, Curr. Opin. Biotechnol. 49 (2017) 57–63.
[22] H. Takano, E. Manabe, M. Hirano, M. Okazaki, J.G. Burgess, N. Nakamura, T. Matsunaga, Development of a rapid isolation procedure for coccolith ultrafine particles produced by coccolithophorid algae, Appl. Biochem. Biotechnol. 39–40 (1993) 239–247.
[23] N.R. Moheimani, A. Isdepsky, J. Lisec, E. Raes, M.A. Borowitzka, Coccolithophorid algae culture in closed photobioreactors, Biotechnol. Bioeng. 108 (2011) 2078–2087.
[24] H. Takano, H. Furu-une, J.G. Burgess, E. Manabe, M. Hirano, M. Okazaki, T. Matsunaga, Production of ultrafine calcite particles by coccolithophorid algae grown in a bisolar reactor supplied with sunlight, Appl. Biochem. Biotechnol. 39–40 (1993) 159–167.
[25] H. Takano, J. Jeon, J.G. Burgess, E. Manabe, Y. Izumi, M. Okazaki, T. Matsunaga, Continuous production of extracellular ultrafine calcite particles by the marine coccolithophorid alga *Pleurochrysis carterae*, Appl. Biochem. Biotechnol. 40 (1994) 946–950.
[26] H. Takano, R. Takei, E. Manabe, J.G. Burgess, M. Hirano, T. Matsunaga, Increased coccolith production by *Emiliania huxleyi* cultures enriched with dissolved inorganic carbon, Appl. Microbiol. Biotechnol. 43 (1995) 460–465.
[27] H. Takano, R. Takei, E. Manabe, T. Matsunaga, Production of coccolith particle by coccolithophorid alga *Emiliania huxleyi*, J. Mar. Biotechnol. 3 (1995) 93–96.
[28] L.K. Medlin, G.L.A. Barker, L. Campbell, J.C. Green, P.K. Hayes, D. Marie, S. Wrieden, D. Valout, Genetic characterization of *Emiliania huxleyi* (Haptophyta), J. Mar. Syst. 9 (1996) 13–31.
[29] J.A. Berges, D.J. Franklin, P.J. Harrison, Evolution of an artificial seawater medium: improvements in enriched seawater, artificial water over the last two decades, J. Phycol. 37 (2001) 1138–1145.
[30] N.A. Nimer, M.J. Merrett, Calcification rate in *Emiliania huxleyi* Lohmann in response to light, nitrate and availability of inorganic carbon, New Phytol. 123 (1993) 673–677.
[31] E. Paasche, Roles of nitrogen and phosphorus in coccolith formation in *Emiliania huxleyi* (prymnesiophyceae), Eur. J. Phycol. 33 (1998) 33–42.
[32] M.J. Merrett, L.F. Dong, N.M. Merrett, Nitrate availability and calcite production in *Emiliania huxleyi* Lohmann, Eur. J. Phycol. 28 (1993) 243–246.
[33] R. Bartal, B. Shi, W.P. Cochlan, E.J. Carpenter, A model system elucidating calcification functions in the phrymnesiophyte *Emiliania huxleyi* reveals dependence of nitrate acquisition on coccoliths, Limnol. Oceanogr. 60 (2015) 149–158.
[34] T.-H. Kim, G. Kim, Changes in seawater N: P ratios in the northwestern Pacific Ocean in response to increasing atmospheric N deposition: results from the East (Japan) Sea, Limnol. Oceanogr. 58 (2013) 1907–1914.
[35] P.L. Blackwelder, R.E. Weiss, K.M. Wilbur, Effects of calcium, strontium and magnesium on the coccolithophorid *Cricosphaera* (Hymenomonas) *carterae*. I. calcification, Mar. Biol. 34 (1976) 11–16.
[36] G. Langer, N. Gussone, G. Nehrke, U. Riesebell, A. Eisenhauer, H. Kuhnert, B. Rost, S. Trimborn, S. Thoms, Coccolith strontium to calcium ratios in *Emiliania huxleyi*: the dependence on seawater strontium and calcium concentrations, Limnol. Oceanogr. 51 (2006) 310–320.
[37] I. Zondervan, The effects of light, macronutrients, trace elements and CO_2 on the production of calcium carbonate and organic carbon in coccolithophores - a review, Deep-Sea Res. Pt. II 54 (2007) 521–537.
[38] W.G. Sunda, S.A. Huntsman, Cobald and zinc interreplacement in marine phytoplankton: biological and geochemical implications, Limnol. Oceanogr. 40 (1995) 1404–1417.
[39] L. Herfort, E. Loste, F. Meldrum, B. Thake, Structural and physiological effects of calcium and magnesium in *Emiliania huxleyi* (Lohmann) Hay and Mohler, J. Struct. Biol. 148 (2004) 307–314.
[40] M. Jeude, B. Dittrich, H. Niederschulte, T. Anderlei, C. Knocke, D. Klee, J. Büchs, Fed-batch mode in shake flasks by slow-release technique, Biotechnol. Bioeng. 95 (2006) 433–445.
[41] E. Paasche, A review of the coccolithophorid *Emiliania huxleyi* (prymnesiophyceae), with particular reference to growth, coccolith formation, and calcification – photosynthesis interactions, Phycologia 40 (2001) 503–529.
[42] P. Westbroek, J.R. Young, K. Linschooten, Coccolith production (biomineralization) in the marine alga *Emiliania huxleyi*, J. Protozool. 36 (1989) 368–373.
[43] L. Mackinder, G. Wheeler, D. Schroeder, U. Riesebell, C. Brownlee, Molecular mechanisms underlying calcification in coccolithophores, Geomicrobiol J. 27 (2010) 585–595.
[44] L.-M. Holtz, S. Thoms, G. Langer, D.A. Wolf-Gladrow, Substrate supply for calcite precipitation in *Emiliania huxleyi*: assessment of different model approaches, J. Phycol. 49 (2013) 417–426.
[45] L.T. Bach, L. Mackinder, K.G. Schulz, G. Wheeler, D.C. Schroeder, C. Brownlee, U. Riesebell, Dissecting the impact of CO_2 and pH on the mechanisms of photosynthesis and calcification in the coccolithohore *Emiliania huxleyi*, New Phytol. 199 (2013) 121–134.
[46] E.T. Buitenhuis, H.J. De Baar, M.J. Veldhuis, Photosynthesis and calcification by *Emiliania huxleyi* (Prymnesiophyceae) as a function of inorganic carbon species, J. Phycol. 35 (1999) 949–959.
[47] L. Herfort, B. Thake, J. Roberts, Acquisition and use of bicarbonate by *Emiliania huxleyi*, New Phytol. 156 (2002) 427–436.
[48] L.-M. Holtz, D.A. Wolf-Gladrow, S. Thoms, Numerical cell model investigating cellular carbon fluxes in *Emiliania huxleyi*, J. Theor. Biol. 364 (2015) 305–315.
[49] R.E. Zeebe and D.A. Wolf-Gladrow, CO_2 in Seawater: Equilibrium Kinetics, Isotopes, 1st edn, Elsevier Science, Amsterdam.
[50] T. Tyrrell, B. Schneider, A. Charalampopoulou, U. Riesebell, Coccolithophores and calcite saturation state in the Baltic and Black Seas, Biogeosciences 5 (2008) 489–494.
[51] K.J. Flynn, D.R. Clark, G. Wheeler, The role of coccolithophore calcification in bioengineering their environment, Proc. R. Soc. B 283 (2016).
[52] S. Richier, S. Fiorini, M.-E. Kerros, P. von Dassow, J.-P. Gattuso, Response of the calcifying coccolithophore *Emiliania huxleyi* to low pH/high pCO_2: from physiology to molecular level, Mar. Biol. 158 (2011) 511–560.
[53] E. Paasche, Reduced coccolith calcite production under light-limited growth: a comparative study of three clones of *Emiliania huxleyi* (Prymnesiophyceae), Phycologia 38 (1999) 508–516.
[54] J.J. Fritz, W.M. Balch, A light-limited continuous culture study of *Emiliania huxleyi*: determination of coccolith detachment and its relevance to cell sinking, J. Exp. Mar. Biol. Ecol. 207 (1996) 127–147.
[55] H.J. Nanninga, T. Tyrrell, Importance of light for the formation of algal blooms by *Emiliania huxleyi*, Mar. Ecol. Prog. Ser. 136 (1996) 195–203.
[56] Garde and Cailliau, The impact of UV-B radiation and different PAR intensities on growth, uptake of 14C, excretion of DOC, cell volume, and pigmentation in the marine *pymnesiophyte Emiliania huxleyi*, J. Exp. Mar. Biol. Ecol. 247 (2000) 99–112.
[57] S. Tong, D.A. Hutchins, K. Gao, Physiological and biochemical responses of *Emiliania huxleyi* to ocean acidification and warming are modulated by UV radiation, Biogeosci. Discuss. (2017) 1–35.
[58] G.N. Harris, D.J. Scanlan, R.J. Geider, Acclimation of *Emiliania huxleyi* (Prymnesiophyceae) to photon flux density, J. Phycol. 41 (2005) 851–862.
[59] J.L. Garrido, C. Brunet, F. Rodríguez, Pigment variations in *Emiliania huxleyi* (CCMP370) as a response to changes in light intensity and quality, Environ. Microbiol. 18 (2016) 4412–4425.
[60] M. Loebl, A.M. Cockshutt, D.A. Campbell, Z.V. Finkel, Physiological basis for high resistance to photoinhibition under nitrogen depletion in *Emiliania huxleyi*, Limnol. Oceanogr. 55 (2010) 2150–2160.
[61] I. Hariskos, T. Rubner, C. Posten, Investigation of cell growth and chlorophyll a content of the coccolithophorid alga *Emiliania huxleyi* by using simple bench-top flow cytometry, J. Bioprocess Biotech. 5 (2015) 234.
[62] J.C. Weissman, R.P. Goebel, J.R. Benemann, Photobioreactor design: mixing, carbon utilization and oxygen accumulation, Biotechnol. Bioeng. 31 (1988) 336–344.
[63] G. Langer, K. Oetjen, T. Brenneis, On culture artefacts in coccolith morphology, Helgol. Mar. Res. 67 (2013) 359–369.
[64] Y. Chisti, Hydrodynamic damage to animal cells, Crit. Rev. Biotechnol. 21 (2001) 67–110.
[65] M.J. Barbosa, R.H. Wijffels Hadiyanto, Overcoming shear stress of microalgae cultures in sparged photobioreactors, Biotechnol. Bioeng. 85 (2004) 78–85.
[66] D.A. Wolf-Gladrow, R.E. Zeebe, C. Klaas, A. Körtzinger, A.G. Dickson, Total alkalinity: the explicit conservative expression and its application to biogeochemical processes, Mar. Chem. 106 (2007) 287–300.
[67] A.G. Dickson, An exact definition of total alkalinity and a procedure for the estimation of alkalinity and total inorganic carbon from titration data, Deep-Sea Res. Pt. A 28 (1981) 609–623.
[68] D.E. Pierrot, D.W. Lewis, MS Excel Program Developed for CO_2 System Calculations. ORNL/CDIAC-105a, Carbon Dioxide Information Analysis Center, Oak Ridge National Laboratory, U.S. Department of Energy, Oak Ridge, Tennessee, 2006.
[69] C. Mehrbach, C.H. Culberson, J.E. Hawley, R.M. Pytkowicx, Measurement of the apparent dissociation constants of carbonic acid in seawater at atmospheric pressure, Limnol. Oceanogr. 18 (1973) 897–907.
[70] F.J. Millero, A.J. Dickson, G. Eischeid, C. Goyet, P. Guenther, K.M. Johnson, R.M. Key, K. Lee, D. Purkerson, C.L. Sabine, R.G. Schottle, D.W. Wallcae, E. Lewis, C.S. Winn, Assessment of the quality of the shipboard measurements of total alkalinity on the WOCE Hydrographic Program Indian Ocean CO_2 survey cruises, Mar. Chem. 63 (1994–1996) 9–20.
[71] A.G. Dickson, Thermodynamics of the dissociation of boric acid in synthetic seawater from 273.15 to 318.15 K, Deep-Sea Res. Pt. A 37 (1990) 755–766.
[72] L.E. Brand, The salinity tolerance of forty-six marine phytoplankton isolates, Estuar. Coast. Shelf S. 18 (1984) 543–556.
[73] S. Boussiba, A.E. Richmond, C-phycocyanin as a storage protein in the blue-green alga *Spirulina platensis*, Arch. Microbiol. 125 (1980) 143–147.
[74] S. Eixler, U. Karsten, U. Selig, Phosphorus storage in *Chlorella vulgaris* (Trebouxiophyceae, Chlorophyta) cells and its dependence on phosphate supply, Phycologia 45 (2006) 53–60.
[75] J.H. Ryther, N. Corwin, T.A. DeBusk, L.D. Williams, Nitrogen uptake and storage by the red alga *Gracilaria tikvahiae* (McLachlan, 1979), Aquaculture 26 (1981) 107–115.
[76] D. Knies, P. Wittmüß, S. Appel, O. Sawodny, M. Ederer, R. Feuer, Modeling and simulation of optimal resource management during the diurnal cycle in *Emiliania huxleyi* by genome-scale reconstruction and an extended flux balance analysis approach, Meta 5 (2015) 659–676.
[77] G.M. Durak, A.R. Taylor, C.E. Walker, I. Probert, C. De Vargas, S. Audic, D. Schroeder, C. Brownlee, G.L. Wheeler, A role for diatom-like silicon transporters in calcifying coccolithophores, Nat. Commun. 7 (2016) 10543.
[78] S.M. Patil, R. Mohan, S. Shetye, S. Gazi, S. Jafar, Morphological variability of *Emiliania huxleyi* in the Inditan sector of the Southern Ocean during the austral summer of 2010, Mar. Micropaleontol. 107 (2014) 44–58.
[79] S.S. Cook, L. Whittock, S.W. Wright, G.M. Hallegraeff, Photosynthetic pigment and genetic differences between two southern ocean morphotypes of *Emiliania huxleyi* (Haptophyta), J. Phycol. 47 (2011) 615–626.
[80] T.Y. Ho, A. Quigg, Z.V. Finkel, A.J. Milligan, K. Wyman, P.G. Falkowski, F.M. Morel, Erratum: the elemental composition of some marine phytoplankton, J. Phycol. 39 (2004) 1145–1159.